

## Iodide substitution in lithium borohydride, LiBH<sub>4</sub>-LiI

Line H. Rude,<sup>a</sup> Elena Groppo,<sup>b</sup> Lene M. Arnbjerg,<sup>a</sup> Dorthe B. Ravnsbæk,<sup>a</sup> Regitze A. Malmkjær,<sup>a</sup> Yaroslav Filinchuk,<sup>a,c,d</sup> Marcello Baricco,<sup>b</sup> Flemming Besenbacher,<sup>e</sup> Torben R. Jensen.<sup>a,\*</sup>

<sup>a</sup> *Center for Materials Crystallography, Interdisciplinary Nanoscience Center and Department of Chemistry, Aarhus University, Langelandsgade 140, DK-8000 Århus C, Denmark.*

<sup>b</sup> *Dipartimento di Chimica I.F.M. and NIS, Università di Torino, Torino, Italy*

<sup>c</sup> *Swiss-Norwegian Beam Lines at ESRF, BP-220, 38043 Grenoble, France*

<sup>d</sup> *Institute of Condensed Matter and Nanosciences, Université Catholique de Louvain, place L. Pasteur 1, B-1348 Louvain-la-Neuve, Belgium*

<sup>e</sup> *Interdisciplinary Nanoscience Center (iNANO) and Department of Physics and Astronomy, Aarhus University, DK-8000 Aarhus C, Denmark.*

Author's e-mail address:

Line H. Rude: [line@inano.au.dk](mailto:line@inano.au.dk)

Elena Groppo: [elena.groppo@unito.it](mailto:elena.groppo@unito.it)

Lene M. Arnbjerg: [lenem@chem.au.dk](mailto:lenem@chem.au.dk)

Dorthe B. Ravnsbæk: [inadr@inano.au.dk](mailto:inadr@inano.au.dk)

Regitze Aagaard Malmkjær: [regitze.aagaard.malmkjaer@post.au.dk](mailto:regitze.aagaard.malmkjaer@post.au.dk)

Yaroslav Filinchuk: [Yaroslav.Filinchuk@uclouvain.be](mailto:Yaroslav.Filinchuk@uclouvain.be)

Marcello Baricco: [marcello.baricco@unito.it](mailto:marcello.baricco@unito.it)

Flemming Besenbacher: [fbe@inano.au.dk](mailto:fbe@inano.au.dk)

Torben R. Jensen: [trj@chem.au.dk](mailto:trj@chem.au.dk)

\* Corresponding author: [trj@chem.au.dk](mailto:trj@chem.au.dk), Tel: +45 8942 3894, Fax: +45 8619 6199

## Abstract

The new concept, anion substitution is explored for possible improvement of hydrogen storage properties in the system LiBH<sub>4</sub>-LiI. The structural chemistry and the substitution mechanism is analyzed using Rietveld refinement of *in situ* synchrotron radiation powder X-ray diffraction (SR-PXD) data, attenuated total reflectance infrared spectroscopy (ATR-IR), differential scanning calorimetry (DSC) and Sieverts measurements. Anion substitution is observed as formation of a solid solution of Li(BH<sub>4</sub>)<sub>1-x</sub>I<sub>x</sub> with a hexagonal structure (space group *P6<sub>3</sub>mc*) similar to the structures of *h*-LiBH<sub>4</sub> and β-LiI. The solid solution has an iodide content in the range from ~0 to >62 mol%. The hexagonal solid solution Li(BH<sub>4</sub>)<sub>1-x</sub>I<sub>x</sub> is stable from below room temperature (*RT*) to the melting point at 330 °C, which is different from the stability of the parent compounds, orthorhombic and hexagonal LiBH<sub>4</sub> and β-LiI. Furthermore, the rehydrogenation properties of the iodide substituted solid solution Li(BH<sub>4</sub>)<sub>1-x</sub>I<sub>x</sub>, measured by the Sieverts method, are improved as compared to those of LiBH<sub>4</sub>. After four cycles of hydrogen release and uptake the Li(BH<sub>4</sub>)<sub>1-x</sub>I<sub>x</sub> solid solution maintains 68% of the calculated hydrogen storage capacity in contrast to LiBH<sub>4</sub>, which maintains only 25% of the storage capacity after two cycles under identical conditions.

*Keywords:* Hydrogen storage; Lithium borohydride; Anion substitution; *In situ* powder X-ray diffraction; Sieverts method; Rehydrogenation; Infrared spectroscopy

## 1. Introduction

One of the greatest challenges of this century is the implementation of a new carbon free energy system. Hydrogen is considered a promising candidate for storage of renewable energy having a specific energy content of 120 MJ/kg, which is almost three times higher than that of gasoline (43 MJ/kg) [1,2].

Metal borohydride materials are receiving increasing interest as potential hydrogen storage materials due to their high volumetric and gravimetric hydrogen densities, *e.g.* lithium borohydride, LiBH<sub>4</sub>, containing  $\rho_m = 18.5$  wt% H<sub>2</sub> [3-5]. However, important physical properties need to be improved, *e.g.* due to high thermal stability, hydrogen release and uptake occur only at unfavourable conditions and the kinetics is often too slow. These challenges have been addressed in several ways, such as design of novel bi-metal borohydrides [6-13], utilization of new reaction pathways (reactive hydride composites) [14-17], and the concept of nanoconfinement, where nano-particles of metal hydrides are infiltrated in porous materials [18,19]. Recently, the concept of anion substitution in borohydrides, *e.g.* halide ion substitution of the complex anion BH<sub>4</sub><sup>-</sup> in LiBH<sub>4</sub> and Ca(BH<sub>4</sub>)<sub>2</sub> was investigated regarding crystal structures [20-24] and lithium ion conductivity [25,26]. The ion conductivity in LiBH<sub>4</sub> is significantly improved for the solid solutions LiBH<sub>4</sub>-LiX, X = Cl, Br, I, and may find applications as solid electrolytes for all-solid-state batteries [25-30]. Fast dissolution of LiCl in the hexagonal phase *h*-LiBH<sub>4</sub>, forming *h*-Li(BH<sub>4</sub>)<sub>0.6</sub>Cl<sub>0.4</sub> at 240 °C, and slow segregation of LiCl from the solid solution forming orthorhombic *o*-Li(BH<sub>4</sub>)<sub>0.9</sub>Cl<sub>0.1</sub> after months at room temperature (*RT*) has been reported [20]. However, only little is known about the rehydrogenation properties of these materials, a subject where anion substitution might have a significant effect.

In this study we focus on the iodide substitution in lithium borohydride. Lithium borohydride exhibits interesting structural chemistry with four known polymorphs [3,31-33], whereof two exist under ambient pressures. The stable *RT* polymorph is orthorhombic *o*-LiBH<sub>4</sub> with space group symmetry *Pnma* (no. 62). At  $T \sim 112$  °C a transformation to the high-temperature hexagonal *h*-LiBH<sub>4</sub> polymorph occurs [31,32,34]. The *h*-LiBH<sub>4</sub> has the space group symmetry *P6<sub>3</sub>mc* (no. 186) and is stable until melting at  $T \sim 268$  °C with decomposition of the melt at  $\sim 467$  °C [6,7].

Lithium iodide,  $\alpha$ -LiI, has a cubic NaCl-type structure with space group  $Fm-3m$  (no. 225), in which the Li and I coordinations are octahedral. However, if the ionic radii are considered, Li and I would be expected to exhibit tetrahedral coordination at  $RT$ , due to the low ratio between the ionic radii,  $r(\text{cation})/r(\text{anion})$ , of 0.25. This is observed in a hexagonal form of LiI, denoted  $\beta$ -LiI, with space group  $P6_3mc$  (no. 186) that exists at  $T < 0$  °C using a substrate to initiate crystal growth [35-39]. Furthermore, a solid solution of LiI and LiBr can stabilize the  $\beta$ -LiI structure up to 80 °C [35]. The  $h$ -LiBH<sub>4</sub> and  $\beta$ -LiI therefore obtain a similar structure.

Here we present the synthesis, crystal structure and physical properties of iodide-substituted lithium borohydride investigated by *in situ* synchrotron radiation powder X-ray diffraction (SR-PXD), attenuated total reflectance infrared spectroscopy (ATR-IR), differential scanning calorimetry (DSC) and the Sieverts method.

## 2. Experimental

Samples were prepared using lithium borohydride, LiBH<sub>4</sub>, (95%, Aldrich) and lithium iodide, LiI, (99.99%, Aldrich) in compositions 1:0.5 (denoted **S1**), 1:0.6 (**S2**) and 1:1 (**S3**). All samples were ball milled in a Fritch Pulverisette no. 4 using the same procedure, *i.e.* high energy ball milling under inert conditions (argon atmosphere) comprised of 60 times 2 min of milling each intervened by 2 min breaks to avoid heating of the sample. The sample to ball ratio was 1:40 and tungsten carbide (WC) vial (80 mL) and balls (10 mm) were used. A fraction (~0.5 g) of samples prepared in the same way as **S1** and **S2** were transferred to corundum crucibles, placed in sealed argon filled quartz tubes and annealed (A) in a furnace kept at a fixed temperature of 280 °C (**S1A**) or 245 °C (**S2A**) for 96 hours. The samples obtained after annealing are denoted **S1A** and **S2A**, respectively. A sample of LiBH<sub>4</sub>-LiI in

composition 1:1 was prepared by hand mixing (HM) in an agate mortar (denoted **S4**). All investigated samples are listed in Table 1.

All sample preparations and handling were performed under inert argon atmosphere in a MBraun Unilab glove box with a recirculation gas purification system and gas/humidity sensors. Oxygen and water levels were kept well below 1 ppm during all operations.

**Table 1** The composition of the investigated samples is given as the molar ratios and as the molar fractions,  $n(\text{LiI})/n(\text{total})$ , and the hydrogen content,  $\rho_m(\text{H}_2)$ , is calculated. The preparation methods are either ball milling (BM), in two cases followed by annealing (A) in argon atmosphere, or hand-mixing in a mortar (HM).

Notation	Materials	Molar ratio	$n(\text{LiI})/n(\text{total})$	Preparation	$\rho_m(\text{H}_2)$
<b>S1</b>	LiBH <sub>4</sub> -LiI	1:0.5	0.334	BM	3.41
<b>S1A</b>	LiBH <sub>4</sub> -LiI	1:0.5	0.335	BM and A <sup>1</sup>	3.41
<b>S2</b>	LiBH <sub>4</sub> -LiI	1:0.6	0.371	BM	3.01
<b>S2A</b>	LiBH <sub>4</sub> -LiI	1:0.6	0.371	BM and A <sup>2</sup>	3.01
<b>S3</b>	LiBH <sub>4</sub> -LiI	1:1	0.500	BM	1.94
<b>S4</b>	LiBH <sub>4</sub> -LiI	1:1	0.500	HM	1.94

<sup>1</sup> 280 °C / 96 h

<sup>2</sup> 245 °C / 96 h

In house powder X-ray diffraction (PXRD) data were collected at *RT* using a SuperNova diffractometer (Oxford diffraction) with microfocus MoK $\alpha$  (0.7093 Å) X-ray source and a CCD Atlas detector at distance 60 mm. Data were collected between 4 and 46.7° 2 $\theta$  with an exposure time of ~180 s. The sample was mounted in a 0.5 mm glass capillary sealed with glue.

*In situ* SR-PXD data for sample **S1** were measured at the beamline BM01A of the Swiss-Norwegian Beam Lines (SNBL), European Synchrotron Radiation Facility (ESRF), Grenoble, France, using a MAR345 image plate detector. The samples were mounted in glass capillaries (o.d. 0.5 mm) sealed with a composite adhesive to prevent contact with air. The

data were collected at a sample-to-detector distance of 240 mm and the capillaries were rotated 20° during the data collection. The X-ray exposure time for each powder pattern was 20 s using a selected wavelength of  $\lambda = 0.709637$  Å. The wavelength and the detector geometry were calibrated using an external standard, LaB<sub>6</sub>. The sample was heated from *RT* to 300 °C with a heating rate of 5 °C/min and subsequently cooled naturally to 26 °C. This procedure was repeated three consecutive times using the same sample.

*In situ* SR-PXD data were measured for **S1A** and **S4** at the MAX-II synchrotron, beamline I711 at MAX-lab, Lund, Sweden with a MAR165 CCD detector system ( $\lambda = 0.907700$  and 0.94608 Å for **S1A** and **S4**, respectively) [40]. The samples were mounted in sapphire (Al<sub>2</sub>O<sub>3</sub>) single crystal tubes (1.09 mm o.d., 0.79 mm i.d.) under argon [41,42]. The X-ray exposure time was 30 s per PXD pattern and the samples were heated from *RT* to 240 °C (**S1A**) or from *RT* to 280 °C (**S4**). The latter sample was kept at 280 °C for 30 min and then heated from 280 to 290 °C. A heating ramp of 5 °C/min was used for all experiments.

All SR-PXD data were integrated using the Fit2D program [43] and analyzed by Rietveld refinement using Fullprof suite [44]. The background was described by linear interpolation between selected points, while Gauss profile functions were used to fit the diffraction peaks. In the refinements, scale factors, unit cell parameters, profile parameters ( $U$ ,  $V$ ,  $W$ ), the overall temperature factor and the background were refined. The structural model for the solid solution Li(BH<sub>4</sub>)<sub>1-x</sub>I<sub>x</sub> was developed from the structures of *h*-LiBH<sub>4</sub> and  $\beta$ -LiI, which are identical except for a displacement along the  $z$ -axis. For the solid solution the individual temperature factors, the occupancies and the atomic  $z$ -parameter for the anion site were additionally refined. Since the temperature factors and the occupancies are correlated, the temperature factors were initially refined with the occupancies fixed to the value of the prepared composition of the sample. Then the temperature factors were fixed and the occupancies were refined.

Differential scanning calorimetry (DSC) was performed on **S3** and **S4** with a Netzsch STA449C Jupiter instrument from *RT* to 430 °C with a heating rate of 1.5 °C/min in helium (purity 4.6) atmosphere. The samples were contained in Al<sub>2</sub>O<sub>3</sub> crucibles.

Infrared spectroscopy measurements were performed for **S2A** using an ATR-IR spectrophotometer (Bruker Alpha equipped with an ATR accessory with Ge crystal), placed in an argon filled glove-box.

Sieverts measurements were recorded for **S1** with a PCTpro 2000 instrument from Hy-Energy [45]. The samples were loaded in an autoclave and sealed in argon atmosphere. Temperature-pressure desorption (TPD) experiments were performed in the temperature range *RT* to 540 °C (0.5 °C/min) in  $p(\text{H}_2) = 1$  bar. Hydrogen absorption data were measured under an initial hydrogen pressure of ca. 100 bar at a temperature of 410 °C for 44 to 64 hours, see Table 2.

### 3. Results and discussion

#### 3.1 Investigation the iodide substitution mechanism by *in situ* SR-PXD

##### *Substitution by mechano-chemical synthesis, ball milling*

In order to study the mechanism of the anion substitution, an *in situ* SR-PXD experiment of a ball milled sample of LiBH<sub>4</sub>-LiI (1:0.5, **S1**), has been performed, see Fig. 1. The sample was heated from *RT* to 300 °C and cooled to 26 °C three times. The first diffractogram, measured at 35 °C, contains Bragg reflections from the solid solution  $h\text{-Li}(\text{BH}_4)_{1-x}\text{I}_x$  with  $x = 0.67$ , and furthermore from  $\alpha\text{-LiI}$  and weak reflections from  $o\text{-LiBH}_4$  ( $V/Z = 54 \text{ \AA}^3$  as reported for pure  $o\text{-LiBH}_4$  [3]). The occupancies of the anions in the solid solution were determined from Rietveld refinements of the data, see details in the experimental section.  $o\text{-LiBH}_4$  transforms at 70 °C to a  $h\text{-Li}(\text{BH}_4)_{1-y}\text{I}_y$  solid solution with a lower volume ( $V/Z = 57.1 \text{ \AA}^3$ ) compared to  $h\text{-Li}(\text{BH}_4)_{1-x}\text{I}_x$  simultaneously present in the sample ( $V/Z = 60.5 \text{ \AA}^3$ ). The reflections are initially

too weak to reliably determine the iodide content, however, the smaller size of the unit cell suggest a lower iodide content.

Upon further heating the intensity of the  $\alpha$ -LiI Bragg reflections decreases and the two solid solutions  $h\text{-Li}(\text{BH}_4)_{1-x}\text{I}_x$  and  $h\text{-Li}(\text{BH}_4)_{1-y}\text{I}_y$  are merging to become a single solid solution of  $h\text{-Li}(\text{BH}_4)_{0.61}\text{I}_{0.39}$  at 264 °C (see Fig. 1B). This composition remains almost constant during the rest of the experiment, *i.e.*  $h\text{-Li}(\text{BH}_4)_{0.61}\text{I}_{0.39}$  is stable from *RT* to temperatures above 300 °C. Thus, the structure of the solid solution is isostructural to both  $h\text{-LiBH}_4$  and  $\beta\text{-LiI}$  with space group symmetry  $P6_3mc$  [35-37].

A plot of the unit cell volumes for the solid solutions  $\text{Li}(\text{BH}_4)_{1-x}\text{I}_x$  observed during the experiment is shown in Fig. 2. This illustrates the coexistence of two solid solutions denoted  $h\text{-Li}(\text{BH}_4)_{1-x}\text{I}_x$  and  $h\text{-Li}(\text{BH}_4)_{1-y}\text{I}_y$  ( $x > y$ ) with different unit cell volume, *i.e.* different degree of substitution, at the beginning of the experiment. Furthermore, the observation of the similar unit cell volumes at 26 °C after each heating and the linear thermal expansion during the second and third heating suggests that  $\alpha\text{-LiI}$  does not segregate from the fully substituted solid solution  $h\text{-Li}(\text{BH}_4)_{0.61}\text{I}_{0.39}$  on the time scale of the experiment. It is also noteworthy that the hexagonal-orthorhombic polymorphic phase transition normally observed at 112 °C for  $\text{LiBH}_4$  [3,31,32,34] is not observed for  $h\text{-Li}(\text{BH}_4)_{1-x}\text{I}_x$  down to *RT*, suggesting that the substitution stabilizes the hexagonal structure.

#### *Anion substitution by thermal treatment*

Anion substitution facilitated by thermal treatment was studied using a ball milled sample of  $\text{LiBH}_4\text{-LiI}$  (1:0.5, **S1A**) annealed at 280 °C for 96 hours. *In situ* SR-PXD data collected at *RT* reveals a single solid solution of  $h\text{-Li}(\text{BH}_4)_{0.73}\text{I}_{0.27}$  with an iodide content of 27 mol%, see Fig. A in the supplementary information. The iodide content was determined with Rietveld refinement and is found to be similar to the initial sample composition.  $h\text{-Li}(\text{BH}_4)_{0.73}\text{I}_{0.27}$  is

observed as a single solid solution during the *in situ* experiment from *RT* to 280 °C. The annealing was performed 14 days prior to measurement of the SR-PXD data shown in Fig. A in supplementary.

A sample of LiBH<sub>4</sub>-LiI (1:0.6, **S2A**) was investigated 27 months after the annealing and the PXD data show Bragg reflections from a single *h*-Li(BH<sub>4</sub>)<sub>1-x</sub>I<sub>x</sub>, *i.e.* no segregation of LiI and *o*-LiBH<sub>4</sub> is observed. However, a small amount (~4 wt%) of a hydrate, LiI·H<sub>2</sub>O is formed, see Fig. B in the supplementary information. The composition of the sample cannot be accurately determined due to insufficient data quality.

This shows that the anion substitution facilitated by thermal treatment (annealing) is stable at *RT* over time.

#### *Substitution by hand mixing in a mortar*

A hand mixed sample of LiBH<sub>4</sub>-LiI (1:1, **S4**) has been prepared and investigated using *in situ* SR-PXD measured from *RT* to 290 °C, see Fig. 3. The first diffractogram, measured at 28 °C, contains Bragg reflections from the starting materials, *o*-LiBH<sub>4</sub> and  $\alpha$ -LiI. The polymorphic phase transformation from *o*-LiBH<sub>4</sub> to *h*-LiBH<sub>4</sub> is observed at 112 °C. Upon further heating the dissolution of LiI into *h*-LiBH<sub>4</sub> is observed as a gradual decrease of the intensity of the  $\alpha$ -LiI reflections, followed by formation of a substituted phase, *h*-Li(BH<sub>4</sub>)<sub>1-x</sub>I<sub>x</sub>. Apparently, two solid solutions of *h*-Li(BH<sub>4</sub>)<sub>1-x</sub>I<sub>x</sub> and *h*-Li(BH<sub>4</sub>)<sub>1-y</sub>I<sub>y</sub> are in equilibrium as observed for the ball milled sample **S1**. At  $T = 219$  °C, the two solid solutions obtain iodide substitution degrees of ~64 mol% and ~0 to 5 mol% and unit cell volumes per formula unit of 61.8 Å<sup>3</sup> and 56.1 Å<sup>3</sup>, respectively. Observation of a larger unit cell volume for the solid solution with higher degree of substitution, agrees well with the larger ionic radii of I<sup>-</sup> (~2.20 Å) as compared to BH<sub>4</sub><sup>-</sup> (~2.03 Å). The reflections from the solid solution *h*-Li(BH<sub>4</sub>)<sub>1-y</sub>I<sub>y</sub>,  $y \sim 0$  to 5 mol%

disappear at  $T = 270$  °C, which is due to formation of a single Li(BH<sub>4</sub>)<sub>1-x</sub>I<sub>x</sub> solid solution as observed for the ball milled sample **S1**, since the reflections from  $\alpha$ -LiI does not reappear.

There is no indication of substitution in the *RT* polymorph of lithium borohydride, *o*-LiBH<sub>4</sub> neither in the cubic  $\alpha$ -LiI in any of the samples. For LiBH<sub>4</sub> this might be explained by the structural dynamics of the structure, *i.e.* the librational motion of the BH<sub>4</sub><sup>-</sup> complex ion, which is significantly larger for the *h*-LiBH<sub>4</sub> than for *o*-LiBH<sub>4</sub> [31,32]. For LiI, the hexagonal structure is energetically favoured if only the binding energy is considered, furthermore, it has been reported that anion substitution of Br<sup>-</sup> stabilizes the hexagonal structure of  $\beta$ -LiI up to  $T \sim 80$  °C [35].

Previously, a trend in the structural chemistry of anion substitution in borohydrides with the heavier halides was reported [21]: a smaller anion tends to dissolve into the compound containing the larger anion, and the structure of the latter tends to be preserved in the obtained solid solution. This trend follows the relative size of the anions,  $\Gamma^- > \text{BH}_4^- > \text{Br}^- > \text{Cl}^-$  [46]. This explains that LiCl dissolves in LiBH<sub>4</sub> but LiBH<sub>4</sub> does not dissolve in LiCl [20]. However, when two solids have identical structures the dissolution process may produce two solid solutions as observed for NaBH<sub>4</sub>-NaCl, where a small amount of NaBH<sub>4</sub> dissolves in NaCl and a larger amount of NaCl dissolves in NaBH<sub>4</sub>. The solid solution LiBH<sub>4</sub>-LiI follows the above mentioned trend since the structures of *h*-LiBH<sub>4</sub> and  $\beta$ -LiI are identical, although, as presented in the experimental section, using different displacements along the *z*-axis of the anion site.

A linear relation between the unit cell volume and the iodide content, *x*, in the observed solid solutions is shown in Fig. 4. The volume of *h*-LiBH<sub>4</sub> at 25 °C has been estimated from the thermal expansion coefficient of *h*-LiBH<sub>4</sub>,  $2.9 \cdot 10^{-4} \text{ K}^{-1}$ , and the volume of  $\beta$ -LiI at 25 °C is reported in the literature [32,35]. The volumes determined for different compositions of Li(BH<sub>4</sub>)<sub>1-x</sub>I<sub>x</sub> are listed in Table A in the supplementary information. The relationship between

the volumes and composition of Li(BH<sub>4</sub>)<sub>1-x</sub>I<sub>x</sub> and β-LiI is found to be linear and follow Vegard's law [47].

The size difference of the ions or atoms being mixed is a crucial parameter for the formation of solid solutions [48]. For LiI-LiX (X=F, Cl, Br) solid solution, a clear correlation between mixing properties and ionic radius of X<sup>-</sup> can be outlined, if the atomic radii of halides for a coordination number equal to 6 are considered [49]: F<sup>-</sup> = 1.33 Å, Cl<sup>-</sup> = 1.81 Å, Br<sup>-</sup> = 1.96 Å and I<sup>-</sup> = 2.20 Å. LiI-LiF binary system shows a complete immiscibility in the solid state, with a eutectic reaction at 413 °C [50]. Because of the immiscibility in the solid state, a positive heat of mixing is expected for this system. Similar behaviour can be observed for LiI-LiCl system [50], but the eutectic temperature is slightly lower (371 °C), suggesting a lower positive enthalpy of mixing. For LiI-LiBr system, the Br<sup>-</sup> anion size is closer to that of I<sup>-</sup>, so that the positive enthalpy of mixing is further reduced and an immiscibility gap becomes evident in the solid state, with a critical temperature of 208 °C [50]. For the BH<sub>4</sub><sup>-</sup> anion, an ionic radius of 2.03 Å has been suggested [51]. So, a significant miscibility is expected for the LiI-LiBH<sub>4</sub> system in the solid state, as evidenced from the obtained results. In fact, a solubility up to about 80% of LiI in LiBH<sub>4</sub> has been recently reported [27].

The enthalpy of mixing in binary solid solutions is also correlated with the volume mismatch of the constituents [48]. This behaviour applies also for alkali halide solid solutions with the rock salt structure and a second-order correlation has been suggested [48]. The observed linear trend of the volume of the unary cell for the solid solutions as a function of composition (see fig. 4) suggests that the volume of mixing is close to zero, so that the Vegard's law is followed by the hexagonal solid solution. As a consequence, a close-to-ideal behaviour is expected for the solution, so that a significant miscibility can be expected in the solid state, because of the entropic contribution. Of course, for the occurrence of a single solid solution it is necessary that any kinetic constraint is overcome by suitable thermal

treatments. As a consequence, during the experiments, the metastable coexistence of two solid solutions has been found, which becomes a single solid solution after heating (see fig. 2). For LiI rich solutions, the presence of the cubic structure in the pure component is expected to limit the solubility. A peritectic reaction is likely to occur close to the melting point of LiI (469 °C), but accurate calorimetric measurements are necessary to reach a full picture of the phase diagram.

### 3.2 Infrared spectroscopy of Li(BH<sub>4</sub>)<sub>1-x</sub>I<sub>x</sub>

In order to study the changes in the vibrational properties of lithium borohydride IR-ATR spectroscopy was performed on an annealed sample of LiBH<sub>4</sub>-LiI (1:0.6, **S2A**), see Fig. 5. The IR-ATR spectrum of as-received *o*-LiBH<sub>4</sub> shows two main sets of IR absorption bands due to B-H stretching (2400-2000 cm<sup>-1</sup> region) and B-H bending (1600 - 800 cm<sup>-1</sup> region) vibrational modes, respectively, as already reported in literature [52-55]. In particular, the Raman spectrum of *o*-LiBH<sub>4</sub> at *RT* has been reported to show a well defined triplet of bands in the B-H stretching region and a doublet in the B-H bending region [52]. The IR spectrum is more complex in the latter region (as evidenced in Fig. 5), because both IR and Raman active bending modes are observed, as well as bands due to combination and overtones [56]. The vibrational spectra of borohydrides are very sensitive to the geometry of the BH<sub>4</sub><sup>-</sup> anions. As a consequence, the orthorhombic to hexagonal polymorphic phase transformation in LiBH<sub>4</sub> leads to a change in the corresponding vibrational spectra, as previously demonstrated by *in situ* Raman spectroscopy measurements as a function of temperature [52]. In particular, upon increasing temperature, the well defined IR absorption bands in both, B-H stretching and bending regions become gradually less defined and when the polymorphic transformation occurs a single and broad band is observed in both regions.

When *o*-LiBH<sub>4</sub> is mixed with  $\alpha$ -LiI (sample **S2A**) the corresponding IR spectrum shows a significant broadening and a decrease in intensity of the IR absorption bands in the B-H stretching region, which can be explained in terms of a polymorphic phase transformation [52]. Furthermore, the IR spectrum in the low frequency region (1500-600 cm<sup>-1</sup>) becomes even more complex than that of the parent *o*-LiBH<sub>4</sub>, and reflects a change in the symmetry of the BH<sub>4</sub><sup>-</sup> anions. Interaction of the BH<sub>4</sub><sup>-</sup> anions with iodide anions leads to small lattice distortion and disordering effects, thus affecting the vibrational spectrum. Finally, it is worth noting that Li-I vibrational modes cannot be observed in the investigated spectral range, *i.e.* the observed changes are not related to unreacted LiI.

### 3.3 Investigation the iodide substitution by differential scanning calorimetry

Differential scanning calorimetry (DSC) measurements were conducted for LiBH<sub>4</sub>-LiI samples (**S3** and **S4**) and compared with a reference sample of as-received LiBH<sub>4</sub>. The data are shown in Fig. 6 for the temperature range *RT* to 430 °C (heating rate 1.5 °C/min). For LiBH<sub>4</sub> two endothermic peaks are observed in the DSC profile, at 115 and 286 °C, respectively. The first signal corresponds to the *o*- to *h*-LiBH<sub>4</sub> polymorphic phase transformation and the second signal to the melting of LiBH<sub>4</sub> [54]. For the hand mixed sample of LiBH<sub>4</sub>-LiI (**S4**) the DSC profile for the first cycle is similar to that of LiBH<sub>4</sub> showing two endothermic peaks, at 114 and 286 °C, respectively, in agreement with the SR-PXD data of **S4** shown in Fig. 3. However, during the second cycle, all DSC signals are significantly weakened, indicating the anion substitution has occurred, resulting in formation of the solid solution *h*-Li(BH<sub>4</sub>)<sub>1-x</sub>I<sub>x</sub>. For the ball milled LiBH<sub>4</sub>-LiI sample (**S2**) one endothermic peak at 322 °C is observed, *i.e.* no signal corresponding to the polymorphic

phase transformation from *o*- to *h*-LiBH<sub>4</sub> is observed and the melting point is shifted towards higher temperatures compared to LiBH<sub>4</sub> in agreement with the SR-PXD data shown in Fig. 1.

### 3.4 Hydrogen storage properties of the solid solution Li(BH<sub>4</sub>)<sub>1-x</sub>I<sub>x</sub>

The rehydrogenation properties of the LiBH<sub>4</sub>-LiI system were investigated using the Sieverts method. The four measured cycles of dehydrogenation for LiBH<sub>4</sub>-LiI (1:0.5, **S1**) are shown in Fig. 7. A slow heating ramp was applied from *RT* to 540 °C (0.5 °C/min) during desorption to follow the dehydrogenation mechanism. The hydrogen absorption measurements were conducted at a constant temperature of 410 °C at  $p(\text{H}_2) = 100$  bar for 44 to 64 hours, see Table 2.

The dehydrogenation profile of the LiBH<sub>4</sub>-LiI (1:0.5, **S1**) system is similar to that of LiBH<sub>4</sub>, see Fig. 7. The hydrogen release is fastest at 450 °C. A total hydrogen release of 3.4 wt% corresponding to the calculated capacity of  $\rho_m(\text{H}_2) = 3.40$  wt% is observed for the LiBH<sub>4</sub>-LiI (1:0.5, **S1**) sample.

After 58 hours of rehydrogenation, at 450 °C and 100 bar hydrogen, a second hydrogen desorption measurement was performed for LiBH<sub>4</sub>-LiI (1:0.5, **S1**) showing a total hydrogen release of 2.7 wt% (79% of the calculated capacity). A third and a fourth desorption was measured after 64 and 44 hours of rehydrogenation, respectively, giving a hydrogen release of 2.6 and 2.3 wt% H<sub>2</sub> (76% and 68% of the calculated capacity). The decrease in hydrogen storage capacity may indicate that the sample is not fully loaded with hydrogen during the absorption, see Table 2.

For LiBH<sub>4</sub>, a total hydrogen release of 13.2 wt% is observed during the first dehydrogenation, *i.e.* 95% of the calculated capacity of  $\rho_m(\text{H}_2) = 13.88$  wt%. A second dehydrogenation was measured for LiBH<sub>4</sub> after 58 hours of rehydrogenation at  $T = 410$  °C,

$p(\text{H}_2) = 100$  bar, showing a release of 3.4 wt%, which is only 25% of the calculated hydrogen storage capacity.

**Table 2.** The calculated gravimetric hydrogen content,  $\rho_m(\text{H}_2)$ , for LiBH<sub>4</sub>-LiI (1:0.5, **S1**) and a reference sample of as-received LiBH<sub>4</sub> are compared to the measured hydrogen content in four desorption cycles using the Sieverts method. The absorption times are shown for each hydrogenation cycle since this has an impact on the amount of gas released from the sample.

Samples	$\rho_m(\text{H}_2)$ /wt%	Des1 /wt%	Abs1 time /h	Des2 /wt%	Abs2 time /h	Des3 /wt%	Abs3 time /h	Des4 /wt%	<b>H<sub>2</sub> Uptake</b> %
LiBH <sub>4</sub>	13.88	13.2	58	3.4	-	-	-	-	<b>25</b>
LiBH <sub>4</sub> -LiI (1:0.5)	3.40	3.4	58	2.7	64	2.6	44	2.3	<b>68</b>

Interestingly, the rehydrogenation seems to occur at more moderate conditions for the Li(BH<sub>4</sub>)<sub>1-x</sub>I<sub>x</sub> solid solution as compared to LiBH<sub>4</sub> [57]. After four cycles of hydrogen release and uptake the LiBH<sub>4</sub>-LiI sample still maintains 68% of the calculated hydrogen storage capacity. The hydrogen storage capacity of LiBH<sub>4</sub> under identical conditions maintains only 25% of the calculated capacity after two cycles. These results indicate that iodide substitution in LiBH<sub>4</sub> stabilises the hydrogenated state and thereby facilitates rehydrogenation.

#### 4. Conclusion

Solid solutions of Li(BH<sub>4</sub>)<sub>1-x</sub>I<sub>x</sub> have been obtained by reacting LiBH<sub>4</sub> with  $\alpha$ -LiI. The substitution of iodide ions for the complex anion BH<sub>4</sub><sup>-</sup> in LiBH<sub>4</sub> can be induced by either elevated temperatures of 245 °C or by mechano-chemical treatment, *i.e.* high energy ball milling.

The substitution has been demonstrated by *in situ* powder X-ray diffraction to form a solid solution obtaining a hexagonal structure similar to the structure of *h*-LiBH<sub>4</sub> and  $\beta$ -LiI and with a substitution degree of up to 62 mol% determined by Rietveld refinement. The

substituted hexagonal compound has a broader stability range (from *RT* to the melting at 330 °C) as compared to both *h*-LiBH<sub>4</sub> and β-LiI. The anion substitution is investigated by attenuated infrared spectroscopy revealing interesting features in the low frequency region and a clear indication of the hexagonal polymorph of LiBH<sub>4</sub> at *RT* in agreement with the synchrotron radiation powder X-ray diffraction and differential scanning calorimetry results. Furthermore, the Sieverts measurements indicate that the rehydrogenation occur more efficiently for the solid solution Li(BH<sub>4</sub>)<sub>1-x</sub>I<sub>x</sub> as compared to LiBH<sub>4</sub> possibly due to stabilisation of the anion substituted material.

### Acknowledgements

The European Commission (contract NMP-2008-261/FLYHY) and the Danish Research Council for Natural Sciences (Danscatt) is thanked for financial support. The work was also supported by the Danish National Research Foundation (Centre for Materials Crystallography), the Danish Strategic Research Council (Centre for Energy Materials) and the Carlsberg Foundation. The access to beam time at the MAX-II synchrotron, Lund, Sweden in the research laboratory MAX-lab is gratefully acknowledged. The authors acknowledge the Swiss-Norwegian Beam Lines (SNBL), European Synchrotron Radiation Facility (ESRF), Grenoble, France, for the allocated beam time.

### References

- [1] U. Eberle, M. Felderhoff, F. Schüth, *Angew. Chem. Int. Ed.* 48 (2009) 6608-6630.
- [2] J. Graetz, *Chem. Soc. Rev.* 38 (2009) 73-82.
- [3] J.P. Soulie, G. Renaudin, R. Černý, K. Yvon, *J. Alloys Compd.* 346 (2002) 200-205.
- [4] L. Schlapbach, A. Züttel, *Nature* 414 (2001) 353-358.
- [5] Y. Filinchuk, D. Chernyshov, V. Dmitriev, *Z. Kristallogr.* 223 (2008) 649-659.
- [6] A. Züttel, A. Borgschulte, S.I. Orimo, *Scripta Mater.* 56 (2007) 823-828.
- [7] H. Li, S.I. Orimo, Y. Nakamori, K. Miwa, N. Ohba, S. Towata, A. Züttel, *J. Alloys Compd.* 446-447 (2007) 315-318.
- [8] H. Hagemann, M. Longhini, J.W. Kaminski, T.A. Wesolowski, R. Černý, N. Penin, M.H. Sørby, B.C. Hauback, G. Severa, C.M. Jensen, *J. Phys. Chem. A* 112 (2008) 7551-

- 7555.
- [9] R. Černý, G. Severa, D.B. Ravnsbæk, Y. Filinchuk, V. d'Anna, H. Hagemann, D. Haase, C.M. Jensen, T.R. Jensen, *J. Phys. Chem. C* 114 (2010) 1357-1364.
- [10] D.B. Ravnsbæk, Y. Filinchuk, Y. Cerenius, H.J. Jakobsen, F. Besenbacher, J. Skibsted, T.R. Jensen, *Angew. Chem. Int. Ed.* 48 (2009) 6659-6663.
- [11] L. Seballos, J.Z. Zhang, E. Rönnebro, J.L. Herberg, E.H. Majzoub, *J. Alloys Compd.* 476 (2009) 446-450.
- [12] D.B. Ravnsbæk, Y. Filinchuk, R. Černý, T.R. Jensen, *Z. Kristallogr.* 225 (2010) 557-569.
- [13] L.H. Rude, T.K. Nielsen, D.B. Ravnsbæk, U. Bösenberg, M.B. Ley, B. Richter, L.M. Arnbjerg, M. Dornheim, Y. Filinchuk, F. Besenbacher, T.R. Jensen, *Phys. Stat. Sol. (b)* Accepted (2011).
- [14] J.Y. Lee, D. Ravnsbæk, Y. Lee, Y. Kim, Y. Cerenius, J. Shim, T.R. Jensen, N.H. Hur, Y.W. Cho, *J. Phys. Chem. C* 113 (2009) 15080-15086.
- [15] U. Bösenberg, S. Doppiu, L. Mosegaard, G. Barkhordarian, N. Eigen, A. Borgschulte, T.R. Jensen, Y. Cerenius, O. Gutfleisch, T. Klassen, M. Dornheim, R. Bormann, *Acta Mater.* 55 (2007) 3951-3958.
- [16] U. Bösenberg, J.W. Kim, D. Gosslar, N. Eigen, T.R. Jensen, J.M. von Colbe, Y. Zhou, M. Dahms, D.H. Kim, R. Günther, Y.W. Cho, K.H. Oh, T. Klassen, R. Bormann, M. Dornheim, *Acta Mater.* 58 (2010) 3381-3389.
- [17] Y.W. Cho, J. Shim, B. Lee, *Calphad* 30 (2006) 65-69.
- [18] T.K. Nielsen, U. Bösenberg, R. Goslawit, M. Dornheim, Y. Cerenius, F. Besenbacher, T.R. Jensen, *ACS Nano* 4 (2010) 3903-3908.
- [19] T.K. Nielsen, F. Besenbacher, T.R. Jensen, *Nanoscale* DOI:10.1039/C0NR00725K (2010).
- [20] L.M. Arnbjerg, D.B. Ravnsbæk, Y. Filinchuk, R.T. Vang, Y. Cerenius, F. Besenbacher, J.E. Jørgensen, H.J. Jakobsen, T.R. Jensen, *Chem. Mater.* 21 (2009) 5772-5782.
- [21] L.H. Rude, Y. Filinchuk, M.H. Sørby, B.C. Hauback, F. Besenbacher, T.R. Jensen, *J. Phys. Chem. C* Accepted (2011).
- [22] J.Y. Lee, Y. Lee, J. Suh, J. Shim, Y.W. Cho, *J. Alloys Compd.* 506 (2010) 721-727.
- [23] L. Mosegaard, B. Møller, J. Jørgensen, Y. Filinchuk, Y. Cerenius, J.C. Hanson, E. Dimasi, F. Besenbacher, T.R. Jensen, *J. Phys. Chem. C* 112 (2008) 1299-1303.
- [24] M. Corno, E. Pinatel, P. Ugliengo, M. Baricco, *J. Alloys Compd.* doi: 10.1016/j.jallcom.2010.10.005 (2010).
- [25] H. Maekawa, M. Matsuo, H. Takamura, M. Ando, Y. Noda, T. Karahashi, S. Orimo, *J. Am. Chem. Soc.* 131 (2009) 894-895.
- [26] M. Matsuo, H. Takamura, H. Maekawa, H. Li, S.I. Orimo, *Appl. Phys. Lett.* 94 (2009) 084103.
- [27] A. Borgschulte, R. Gremaud, S. Kato, N.P. Stadie, A. Remhof, A. Züttel, M. Matsuo, S.I. Orimo, *Appl. Phys. Lett.* 97 (2010) 031916.
- [28] H. Oguchi, M. Matsuo, J.S. Hummelshøj, T. Vegge, J.K. Nørskov, T. Sato, Y. Miura, H. Takamura, H. Maekawa, S.I. Orimo, *Appl. Phys. Lett.* 94 (2009) 141912.
- [29] M. Matsuo, T. Sato, Y. Miura, H. Oguchi, Y. Zhou, H. Maekawa, H. Takamura, S.I. Orimo, *Chem. Mater.* 22 (2010) 2702-2704.
- [30] M. Matsuo, A. Remhof, P. Martelli, R. Caputo, M. Ernst, Y. Miura, T. Sato, H. Oguchi, H. Maekawa, H. Takamura, A. Borgschulte, A. Züttel, S.I. Orimo, *J. Am. Chem. Soc.* 131 (2009) 16389-16391.
- [31] M.R. Hartman, J.J. Rush, T.J. Udovic, R.C. Bowman Jr, S.J. Hwang, *J. Solid State Chem.* 180 (2007) 1298-1305.
- [32] Y. Filinchuk, D. Chernyshov, R. Černý, *J. Phys. Chem. C* 112 (2008) 10579-10584.

- [33] Y. Filinchuk, D. Chernyshov, A. Nevidomskyy, V. Dmitriev, *Angew. Chem. Int. Ed.* 47 (2008) 529-532.
- [34] V. Dmitriev, Y. Filinchuk, D. Chernyshov, A.V. Talyzin, A. Dzwilewski, O. Andersson, B. Sundqvist, A. Kurnosov, *Phys. Rev. B* 77 (2008) 174112.
- [35] D. Fischer, A. Müller, M. Jansen, *Z. Anorg. Allg. Chem.* 630 (2004) 2697–2700.
- [36] B. Wassermann, W. Hönl, T.P. Martin, *Solid State Commun.* 65 (1988) 561–564.
- [37] W. Rühl, *Z. Physik* 143 (1956) 591–604.
- [38] D.C. Johnson, *Nature* 454 (2008) 174–175.
- [39] Y. Liebold-Ribeiro, D. Fischer, M. Jansen, *Angew. Chem. Int. Ed.* 47 (2008) 4428-4431.
- [40] Y. Cerenius, K. Stahl, L.A. Svensson, T. Ursby, A. Oskarsson, J. Albertsson, A. Liljas, *J. Synchrotron Radiat.* 7 (2000) 203–208.
- [41] L. Mosegaard, B. Møller, J.E. Jørgensen, U. Bösenberg, M. Dornheim, J.C. Hanson, Y. Cerenius, G.S. Walker, H.J. Jakobsen, F. Besenbacher, T.R. Jensen, *J. Alloys Compd.* 446-447 (2007) 301-305.
- [42] T.R. Jensen, T.K. Nielsen, Y. Filinchuk, J.E. Jørgensen, Y. Cerenius, E.M. Gray, C.J. Webb, *J. Appl. Cryst.* 43 (2010) 1456-1463.
- [43] A.P. Hammersley, S.O. Svensson, M. Hanfland, A.N. Fitch, D. Hausermann, *High Pressure Res* 14 (1996) 235–248.
- [44] J. Rodriguez-Carvajal, FULLPROF SUITE: LLB Sacley & LCSIM Rennes, France, 2003.
- [45] PCTPro-2000 - Calorimetry and Thermal Analysis, [Http://Www.setaram.com/PCTPro-2000.htm](http://www.setaram.com/PCTPro-2000.htm) (2011).
- [46] Y. Filinchuk, H. Hagemann, *Eur. J. Inorg. Chem.* 20 (2008) 3127-3133.
- [47] L. Vegard, *Z. Phys. A: Hadrons Nucl.* 5 (1921) 17–26.
- [48] P.K. Davies, A. Navrotsky, *J. Solid State Chem.* 46 (1983) 1–22.
- [49] R.D. Shannon, *Acta Cryst A* 32 (1976) 751-767.
- [50] FACT Sage Database [Www.crct.polymtl.ca/Fact](http://www.crct.polymtl.ca/Fact) (2011).
- [51] C.W.F.T. Pistorius, *Z. Phys Chem., Neue Folge* 88 (1974) 253.
- [52] S. Gomes, H. Hagemann, K. Yvon, *J. Alloys Compd.* 346 (2002) 206–210.
- [53] S.I. Orimo, Y. Nakamori, J.R. Eliseo, A. Züttel, C.M. Jensen, *Chem. Rev.* 107 (2007) 4111-4132.
- [54] S.I. Orimo, Y. Nakamori, A. Züttel, *Mater. Sci. Eng., B* 108 (2004) 51–53.
- [55] H. Hagemann, Y. Filinchuk, D. Chernyshov, W. Van Beek, *Phase Transitions* 82 (2009) 344–355.
- [56] K.B. Harvey, N.R. McQuaker, *Can. J. Chem.* 49 (1971) 3282–3286.
- [57] A. Züttel, P. Wenger, S. Rentsch, P. Sudan, P. Mauron, C. Emmenegger, *J. Power Sources* 118 (2003) 1–7.

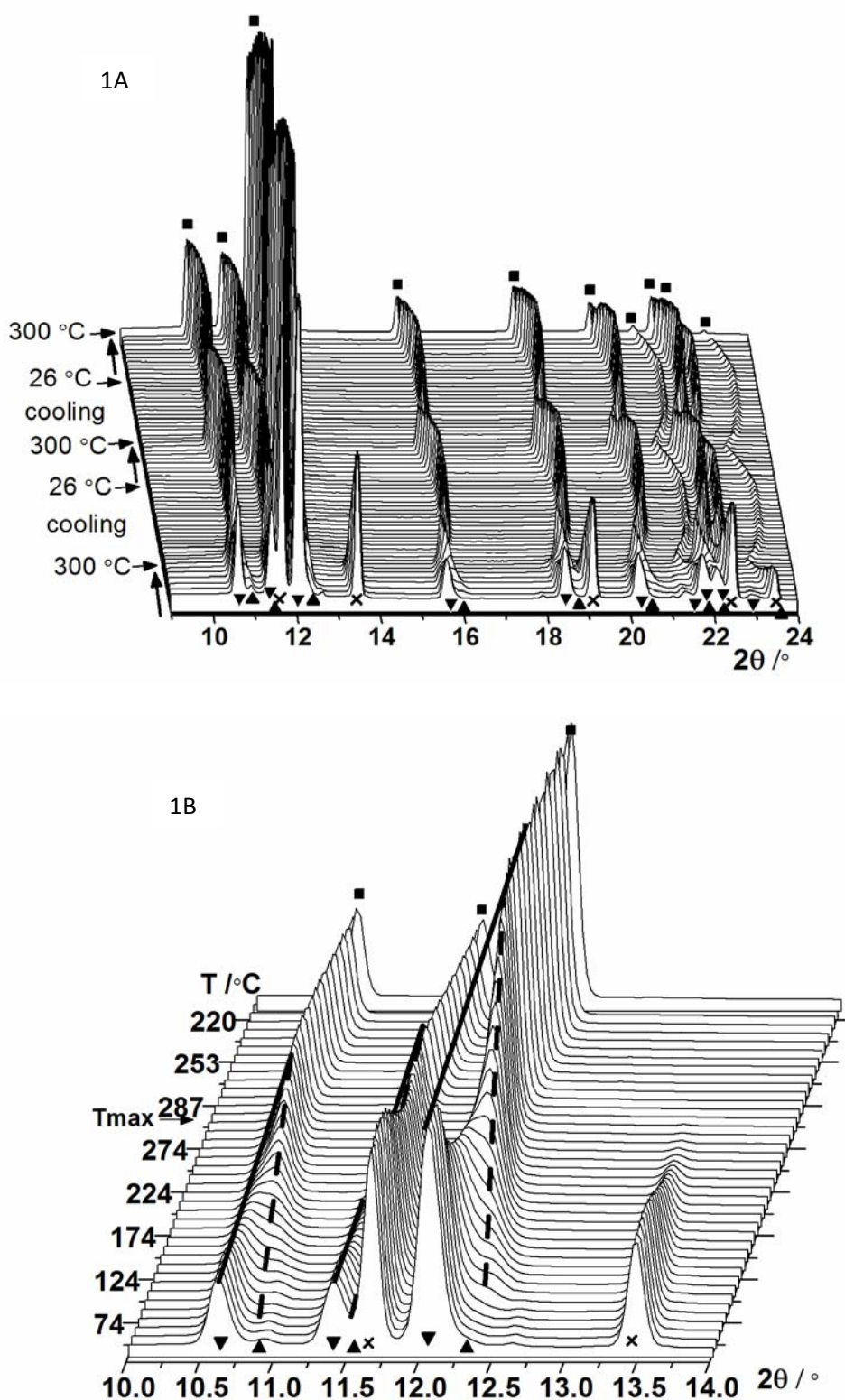


**Fig. 1.** (A) *In situ* SR-PXD data for a ball milled sample of LiBH<sub>4</sub>-LiI (1:0.5, S1) measured at ESRF BM01A ( $\lambda = 0.709637 \text{ \AA}$ ). The sample was heated from RT to 300 °C three times and cooled to 26 °C between each consecutive heating (5 °C/min). Symbols: ×  $\alpha$ -LiI, ▼  $h$ -Li(BH<sub>4</sub>)<sub>1-x</sub>I<sub>x</sub>, ▲  $h$ -Li(BH<sub>4</sub>)<sub>1-y</sub>I<sub>y</sub>, ■  $h$ -Li(BH<sub>4</sub>)<sub>0.61</sub>I<sub>0.39</sub>. (B) Enlarged section of the *in situ* SR-PXD data shown in Fig. 1A in the 2θ region 10 to 14° and temperature region RT to 220 °C of the first heating.

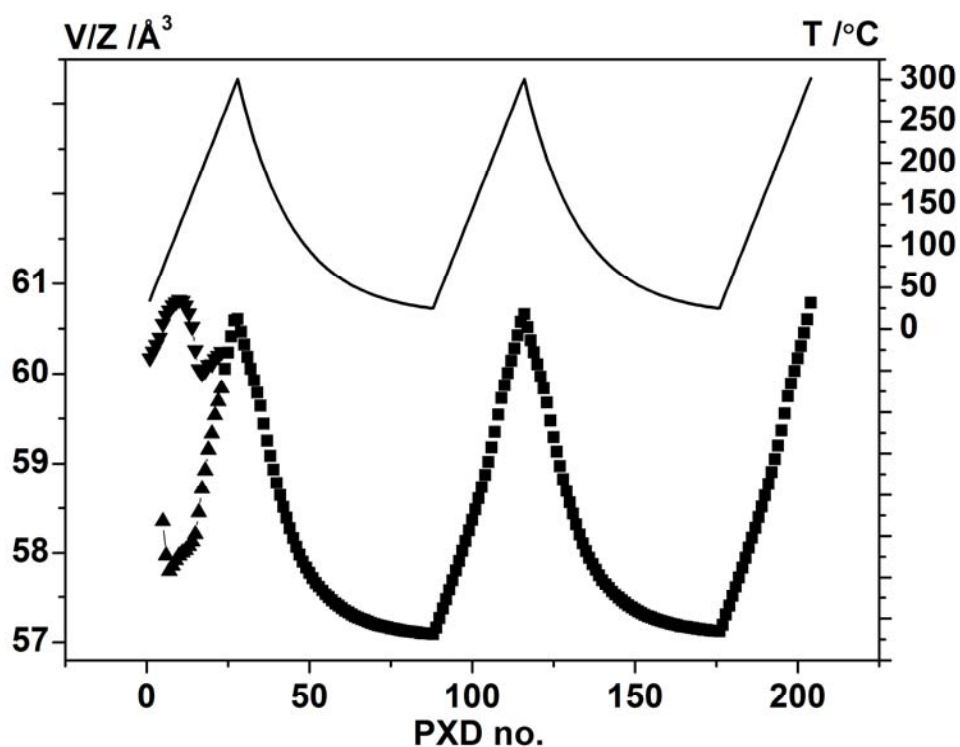


**Fig. 2.** The unit cell volumes for the two solid solutions  $h\text{-Li}(\text{BH}_4)_{1-x}\text{I}_x$  and  $h\text{-Li}(\text{BH}_4)_{1-y}\text{I}_y$  and the fully substituted sample  $h\text{-Li}(\text{BH}_4)_{0.61}\text{I}_{0.39}$  determined from Rietveld refinements of the data shown in Fig. 1A and plotted as a function of PXD no., while the temperature has been cycled. Notice the formation of two solid solutions at the beginning of the first cycle. Symbols: ▼  $h\text{-Li}(\text{BH}_4)_{1-x}\text{I}_x$ , ▲  $h\text{-Li}(\text{BH}_4)_{1-y}\text{I}_y$ , ■  $h\text{-Li}(\text{BH}_4)_{0.61}\text{I}_{0.39}$ . The solid line shows the corresponding temperature.

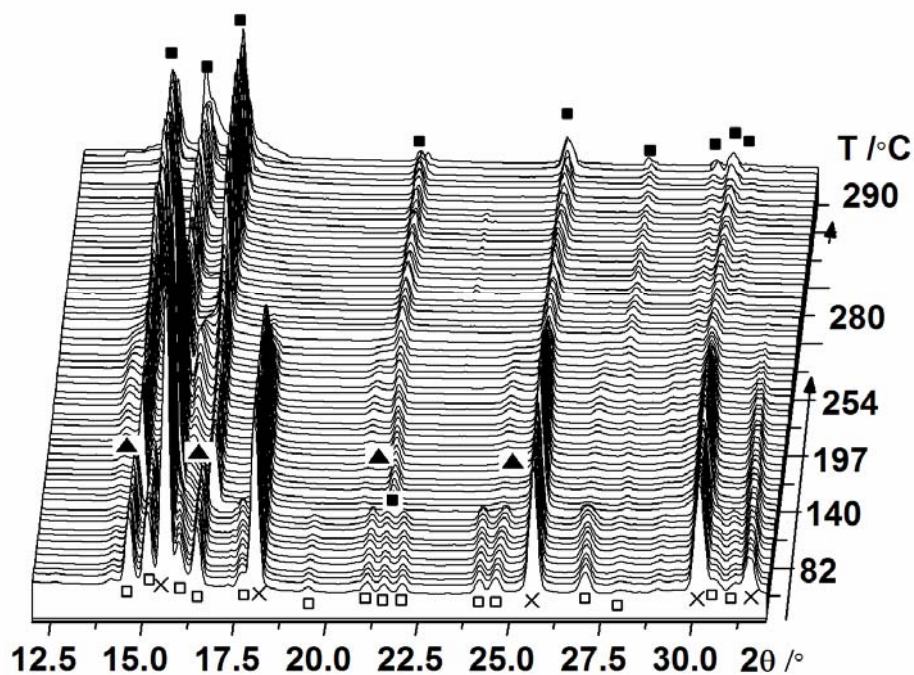


**Fig. 3.** *In situ* SR-PXD data measured at MAX-Lab ( $\lambda = 0.94608 \text{ \AA}$ ) for a hand mixed sample of LiBH<sub>4</sub>-LiI (1:1, S4). The sample was heated from *RT* to 280 °C, kept at a constant temperature of 280 °C for 30 min, and then heated from 280 to 290 °C (heating rate 5 °C/min). Symbols:  $\times$   $\alpha$ -LiI,  $\square$  *o*-LiBH<sub>4</sub>,  $\blacksquare$  *h*-Li(BH<sub>4</sub>)<sub>1-x</sub>I<sub>x</sub>,  $\blacktriangle$  *h*-Li(BH<sub>4</sub>)<sub>1-y</sub>I<sub>y</sub>.

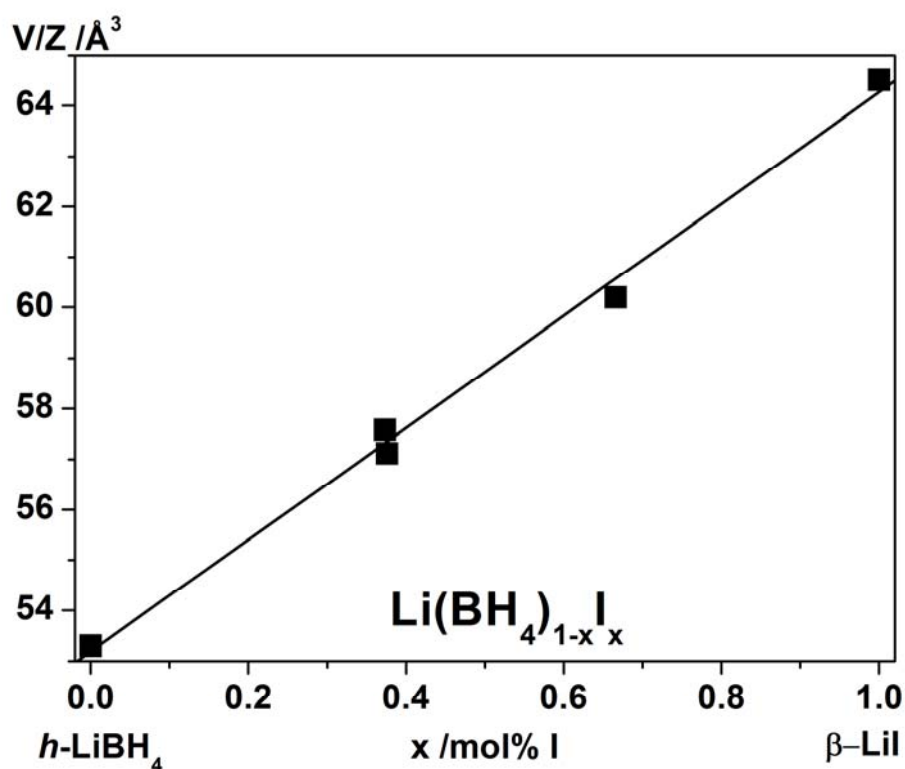


**Fig. 4.** Unit cell volume as a function of the composition of  $\text{Li}(\text{BH}_4)_{1-x}\text{I}_x$ . The values are determined from Rietveld refinements of SR-PXD data measured at *RT* for sample **S1**, see Table A in the supplementary information. The volume of *h*-LiBH<sub>4</sub> at 25 °C is estimated from the thermal expansion coefficient ( $2.9 \cdot 10^{-4} \text{ K}^{-1}$ ) [32] and the volume of  $\beta$ -LiI at 25 °C is given in the literature [35].

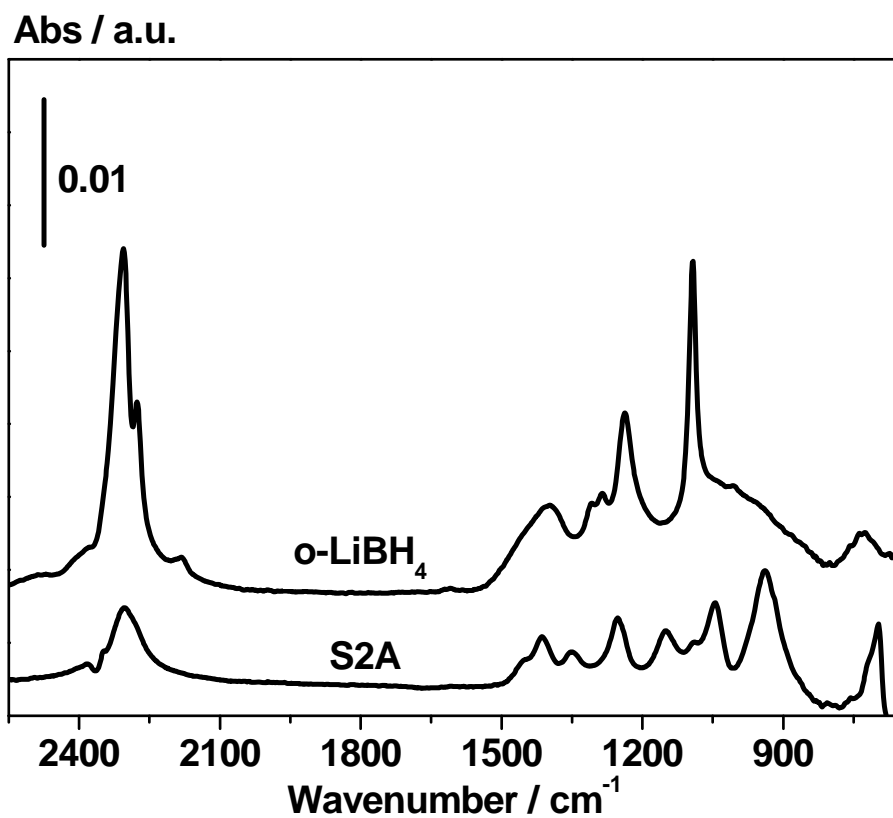
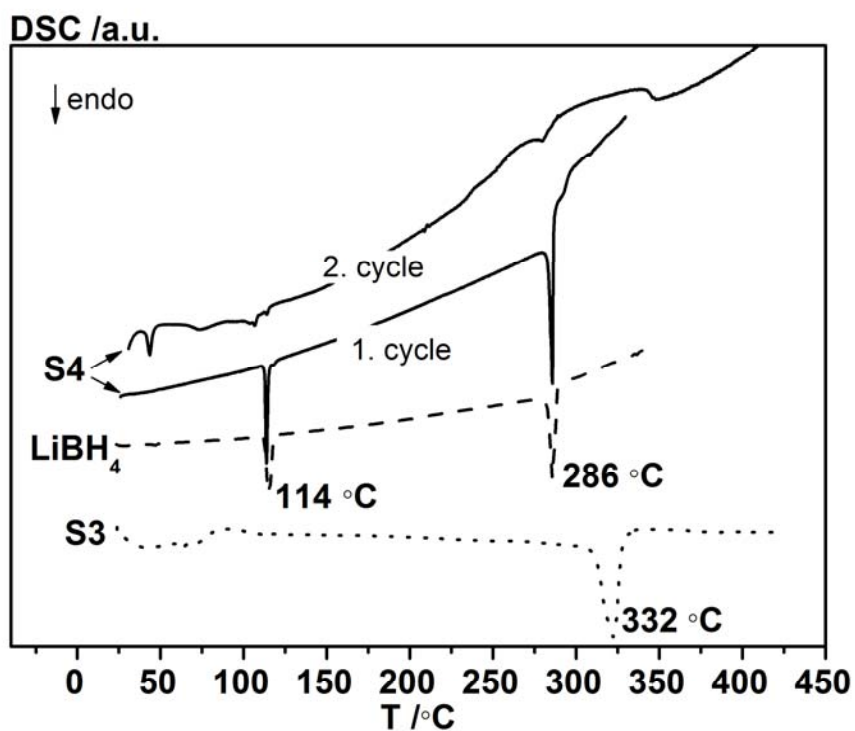
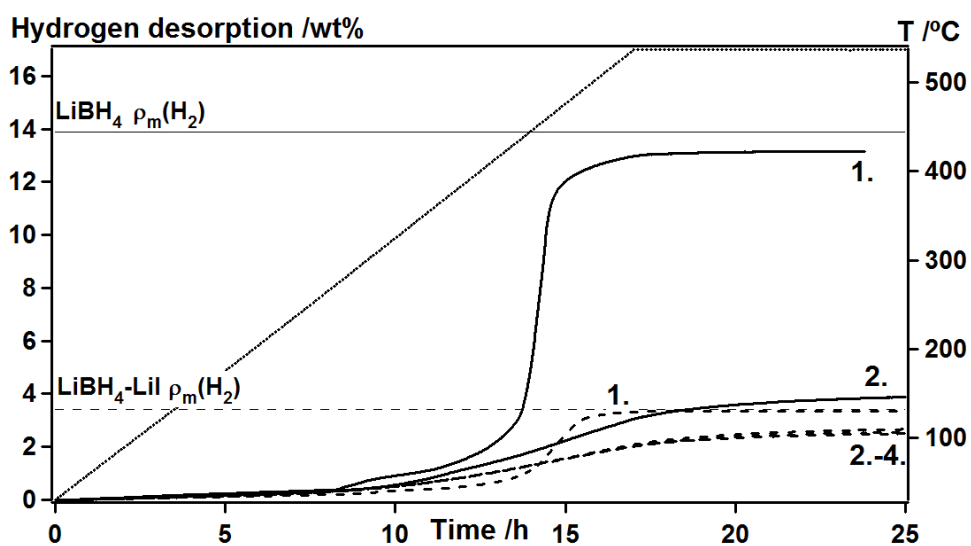


Fig. 5. IR spectra collected in ATR mode (Ge crystal) for LiBH<sub>4</sub> as received (top) and sample S2A (1:0.6, bottom)



**Fig. 6.** Differential Scanning Calorimetry (DSC) conducted from *RT* to 430 °C (heating rate 1.5 °C/min) for LiBH<sub>4</sub>-LiI hand mixed (1:1, **S4**, solid lines), LiBH<sub>4</sub>-LiI ball milled (1:1, **S3**, dots) and a reference sample of LiBH<sub>4</sub> (dashes). For LiBH<sub>4</sub>-LiI hand mixed (1:1, **S4**, solid lines) two cycles have been measured and they are marked 1. cycle and 2. cycle in the figure.



**Fig. 7.** Temperature-pressure desorption measurement by Sieverts method conducted from *RT* to 540 °C (heating rate 0.5 °C/min) for LiBH<sub>4</sub> (solid lines, 1. and 2. desorption) and LiBH<sub>4</sub>-LiI ball milled (1:0.5, **S1**, dashed lines, 1.-4. desorption). The horizontal lines are the calculated hydrogen storage content. The temperature profile is shown as dots.